Inorg. Chem. **2005**, *44*, 9225–9231

Transformation from a 2D Stacked Layer to 3D Interpenetrated Framework by Changing the Spacer Functionality: Synthesis, Structure, Adsorption, and Magnetic Properties

Tapas Kumar Maji, Masaaki Ohba, and Susumu Kitagawa*

Department of Synthetic Chemistry and Biological Chemistry, Graduate School of Engineering, Kyoto University, Katsura, Nishikyo-ku, Kyoto 615-8510, Japan

Received May 24, 2005

Two novel coordination polymers of Cu(II), viz. $[Cu(bipy)(1,4\text{-napdc})(H_2O)_2]_n$ (**1**) and $\{[Cu(bpe)_{1.5}(1,4\text{-napdc})](H_2O)\}_n$ (**2**) (bipy = 4,4′-bipyridine; bpe = 1,2-bis(4-pyridyl)ethane; 1,4-napdc^{2-} = 1,4-naphthalenedicarboxylate), have been synthesized and structurally characterized by changing only the pillar motifs. Both the compounds crystallize by slow evaporation from the ammoniacal solution of the as-synthesized solid. Framework **1** crystallizes in monoclinic crystal system, space group $P2/n$ (No. 13), with $a = 11.028(19)$ Å, $b = 11.16(3)$ Å, $c = 7.678(13)$ Å, $\beta = 103.30(5)°$, and $Z = 2$. Framework **2** crystallizes in triclinic system, space group, $P\bar{1}$ (No. 2), $a = 10.613(4)$ Å, $b = 10.828(10)$ Å, $c = 13.333(9)$ Å, $\alpha = 85.25(9)°$, $\beta = 82.59(6)°$, $\gamma = 60.37(5)°$, and $Z = 2$. The structure determination reveals that **1** has a 2D network based on rectangular grids, where each Cu(II) is in 4 + 2 coordination mode. The 2D networks stacked in a staggered manner through the π–π interaction to form a 3D supramolecular network. In the case of **2**, a $\{Cu(bpe)_{1.5}\}_n$ ladder connected by 1,4-napdc^{2-} results a 2D cuboidal bilayer network and each bilayer network is interlocked by two adjacent identical network (upper and lower) forming 3-fold interpenetrated 3D framework with small channel along the *c*-axis, which accommodates two water molecules. The TGA and XRPD measurements reveal that both the frameworks are stable after dehydration. Adsorption measurements (N_2, CO_2, and different solvents, like H_2O, MeOH, etc.) were carried out for both frameworks. Framework **1** shows type-II sorption profile with N_2 in contrast to H_2O and MeOH, which are chemisorbed in the framework. In case of **2**, only H_2O molecules can diffuse into the micropore, whereas N_2, CO_2, and MeOH cannot be adsorbed, as corroborated by the smaller channel aperture. The low-temperature (300–2 K) magnetic measurement of **1** and **2** reveals that both are weakly antiferromagnetically coupled ($J = -1.85$ cm^{-1}, $g = 2.02$; $J = -0.153$ cm^{-1}, $g = 2.07$), which is correlated by the magnetic pathway to the corresponding structure.

Introduction

The prospect of generating new materials with interesting topology and technologically useful functions provides significant motivation for the recent surge of research interest in organic−inorganic hybrid frameworks.[1] It is well-known that choice of bridging ligands containing appropriate coordination sites linked to the connectors (metal ions) which can adopt different geometry is especially crucial to the construction of desirable framework.[2] By the precise control of the properties of the spacers, such as the shape, functionality, flexibility, length, and symmetry, a remarkable class of materials containing diverse architectures and functions can be obtained.[3] The combination of metal ions and bridging ligands containing different dicarboxylates or rigid and flexible pillars (pyridyl containing) or both can allow the formation of coordination networks possessing permanent porosity and high thermal stability, which are useful for the

* To whom correspondence should be addressed. E-mail: kitagawa@sbchem.kyoto-u.ac.jp. Fax: (+81) 75-383-2732.

(1) (a) Batten, S. R.; Robson, R. *Angew. Chem., Int. Ed.* **1998**, *37*, 1460. (b) Kitagawa, S.; Kitaura, R.; Noro, S.-I. *Angew. Chem., Int. Ed.* **2004**, *43*, 2334. (c) Yaghi, O. M.; O'Keeffe, M.; Ockwig, N. W.; Chae, H. K.; Eddaoudi, M.; Kim, J. *Nature* **2003**, *423*, 705. (d) Janiak, C. *Dalton Trans.* **2003**, 2781. (e) Eddaoudi, M.; Moler, D. B.; Li, H.; Chen. B.; Reineke, T. M.; O'Keeffe, M.; Yaghi, O. M. *Acc. Chem. Res.* **2001**, *34*, 319.

(2) (a) Lehn, J.-M. *Supramolecular Chemistry-Concepts and Perspectives*; VCH: Weinheim, Germany, 1995. (b) Hagrman, P. J.; Hagrman, D.; Zubieta, J. *Angew. Chem., Int. Ed.* **1999**, *38*, 2638. (c) Moulton, B.; Zaworotko, M. J. *Chem. Rev.* **2001**, *101*, 1629. (d) Swiegers, G. F.; Malefetse, T. J. *Chem. Rev.* **2000**, *100*, 3483.

10.1021/ic050835g CCC: $30.25
Published on Web 10/27/2005

ion exchange,[4] separation,[5] chemisorption,[6] gas storage,[7] catalysis,[8] magnetism,[9] optoelectronic,[10] and luminescence properties.[11] For successful performance of porous functions, robustness and thermal stability of the frameworks are essential. Moreover, there are challenges dealing with the access to the pores: (1) As the length of the spacer increases, interpenetration or interdigitation inhibits to the access of pore. (2) There is thermal instability of the whole framework upon removal of the guest. However, recently, some observations were reported that interpenetrated frameworks have permanent porosity and undergo dynamic structural transformation to exhibit porous functionalities, but still this is in the primitive stage.[12−16] On the other hand, amorphous-to-crystal or crystal-to-crystal transformation triggered by guest exchange, representing the 3rd generation of porous frameworks, are the most exciting observations in porous coordination polymer.[17−25] Furthermore, ordered porous materials capable of selective sorption of certain gas and solvent molecules would be useful in sensing and separation, but few examples are known.[26,27] Herein in this paper we report the synthesis, uncommon crystallization procedure, and structures of two novel architectures of Cu(II), [Cu(bipy)-(1,4-napdc)$(H_2O)_2]_n$ (**1**) and $\{([Cu(bpe)_{1.5}(1,4\text{-napdc})](H_2O)\}_n$ (**2**) (bipy = 4,4′-bipyridine; bpe = 1,2-bis(4-pyridyl)ethane; 1,4-napdc^{2-} = 1,4-naphthalenedicarboxylate), along with their selective sorption properties and low-temperature magnetic study. We change here only the pillar module, from bipy, rigid and rodlike, to the more longer and conformationally flexible bpe ligand. The structure determination reveals that **1** is a 2D rectangular grid, which stacked in a staggered manner through $\pi-\pi$ interactions forming a 3D supramolecular framework, whereas **2** is a 2D bilayer network with three bilayer networks mutually interpenetrated forming a 3D framework. This is an unprecedented network transformation (Scheme 1) from a simple modulation in the spacer lengths or chemical functionality or flexibility, which simultaneously affects their topology as well as molecular properties.

Scheme 1. Simplified Representation of the Network Topology of **1** and **2**

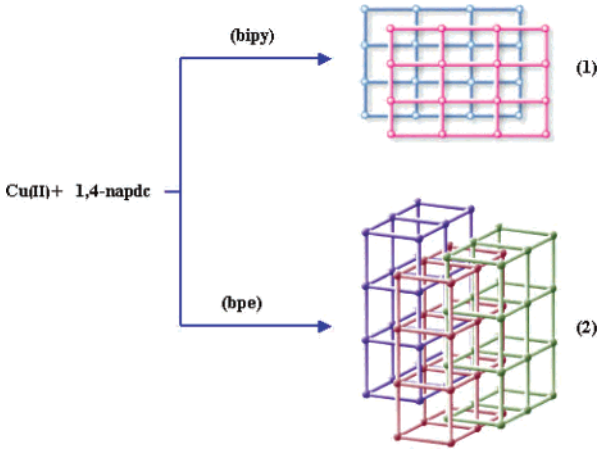

Experimental Section

Materials. All the reagents and solvents employed were commercially available and used as supplied without further purification. $Cu(NO_3)_2{\cdot}2H_2O$ and 1,2-bis(4-pyridyl)ethane were obtained from the Aldrich Co., and 4,4′-bipyridine and naphthalene-1,4-dicarboxylic acid were obtained from Tokyo Kasei Industrial.

(3) (a) Yaghi, O. M.; Li, H.; Davis, C.; Richardson, D.; Groy, T. L. *Acc. Chem. Res.* **1998**, *31*, 474. (b) Evans, O. R.; Lin. W. *Acc. Chem. Res.* **2002**, *35*, 511. (c) Bourne, S. A.; Lu, J.; Mondal, A.; Moulton, B.; Zaworotko, M. J. *Angew. Chem., Int. Ed.* **2001**, *40*, 2011. (d) Noro, S. i.; Kitaura, R.; Kondo, M.; Kitagawa, S.; Ishii, T.; Matsuzaka, H.; Yamashita, M. *J. Am. Chem. Soc.* **2002**, *124*, 2568. (e) Foster, P. M.; Eckert, J.; Chang, J.-S.; Park, S.-E.; Ferey, G.; Cheetham, A. K. *J. Am. Chem. Soc.* **2003**, *125*, 1309.

(4) (a) Pan, L.; Woodlock, E. B.; Wang, X.; Lam, K.-C.; Rheingold, A. L. *Chem. Commun.* **2001**, 1762. (b) Min, K. S.; Suh, M. P. *J. Am. Chem. Soc.* **2000**, *122*, 6834.

(5) (a) Dybtsev, D. N.; Chun, H.; Yoon, S. H.; Kim, D.; Kim, K. *J. Am. Chem. Soc.* **2004**, *126*, 32. (b) Kuznicki, S. M.; Bell, V. A.; Nair, S.; Hillhouse, H. W.; Jacubinas, R. M.; Braunbarth, C. M.; Toby, B. H.; Tsapatsis, M. *Nature* **2001**, *412*, 720.

(6) Yaghi, O. M.; Li, H.; Groy, T. L. *J. Am. Chem. Soc.* **1996**, *118*, 9096.

(7) (a) Noro, S.-I.; Kitagawa, S.; Kondo, M.; Seki, K. *Angew. Chem., Int. Ed.* **2000**, *39*, 2082. (b) Kondo, M.; Okubo, T.; Asami, A.; Noro, S.-I.; Yoshitomi, T.; Kitagawa, S.; Ishii, T.; Matsuzaka, H.; Seki, K. *Angew. Chem., Int. Ed.* **1999**, *38*, 140. (c) Kondo, M.; Yoshitomi, T.; Seki, K.; Matsuzaka, H.; Kitagawa, S. *Angew. Chem., Int. Ed. Engl.* **1997**, *36*, 1725. (d) Rosi, N. L.; Eckert, J.; Eddaoudi, M.; Vodak, D. T.; Kim, J.; O'Keeffe, M.; Yaghi, O. M. *Science* **2003**, *300*, 1127.

(8) (a) Pan, L.; Liu, H.; Lei, X.; Huang, X.; Olson, D. H.; Turro, N. J.; Li, J. *Angew. Chem., Int. Ed.* **2003**, *42*, 542. (b) Fujita, M.; Kwon, Y. J.; Washizu, S.; Ogura, K. *J. Am. Chem. Soc.* **1994**, *116*, 1151.

(9) (a) Halder, G. H.; Kepert, C. J.; Moubaraki, B.; Murray, K. S.; Cashion, J. D. *Science* **2002**, *298*, 1762. (b) Sain, S.; Maji, T. K.; Mostafa, G.; Lu, T.-H.; Ray Chaudhuri, N. *New. J. Chem.* **2003**, *27*, 185. (c) Zeng, M.-H.; Zhang, W.-X.; Sun, X.-Z.; Chen, X.-M. *Angew. Chem., Int. Ed.* **2005**, *44*, 3079. (d) Maji, T. K.; Sain, S.; Mostafa, G.; Lu, T.-H, Ribas, J.; Monfort, M.; Ray Chaudhuri, N. *Inorg. Chem.* **2003**, *42*, 709.

(10) (a) Lin, W.; Wang, Z.; Ma, L. *J. Am. Chem. Soc.* **1999**, *121*, 11249. (b) Evans, O. R.; Xiong, R.; Wang, Z.; Wong, G. K.; Lin, W. *Angew. Chem., Int. Ed.* **1999**, *38*, 536.

(11) (a) Tao, J.; Yin, X.; Wei, Z.-B.; Huang, R.-B.; Zheng, L.-S. *Eur. J. Inorg. Chem.* **2004**, 125. (b) Luo, J.; Hong, M.; Wang, R.; Cao, R.; Han, L.; Lin, Z. *Eur. J. Inorg. Chem.* **2003**, 2705. (c) Fun, H.-K, Sundara Raj, S. S.; Xiong, R.-G.; Zuo, J.-L.; Yu, Z.; You, X.-Z. *J. Chem. Soc., Dalton Trans.* **1999**, 1915.

(12) (a) Kitaura, R.; Seki, K.; Akiyama, G.; Kitagawa, S. *Angew. Chem., Int. Ed.* **2003**, *42*, 428. (b) Kondo, M.; Shimamura, M.; Noro, S.-I.; Minakoshi, S.; Asami, A.; Seki, K.; Kitagawa, S. *Chem. Mater.* **2000**, *12*, 1288.

(13) (a) Reineke, T. M.; Eddaoudi, M.; Moler, D.; O'Keeffe, M.; Yaghi, O. M. *J. Am. Chem. Soc.* **2000**, *122*, 4843. (b) Chen, B.; Eddaoudi, M.; Hyde, S. T.; O'Keeffe, M.; Yaghi, O. M. *Science* **2001**, *291*, 1021.

(14) Seki, K. *Phys. Chem. Chem. Phys.* **2002**, *4*, 1968.

(15) Kesanli, B.; Cui, Y.; Smith, M. R.; Bittner, E. W.; Bockrath, B. C.; Lin, W. *Angew. Chem., Int. Ed.* **2005**, *44*, 72.

(16) Biradha, K.; Fujita, M. *Angew. Chem., Int. Ed.* **2002**, *41*, 3392.

(17) (a) Uemura, K.; Kitagawa, S.; Kondo, M.; Fukui, K.; Kitaura, R.; Chang, H.-C.; Mizutani, T. *Chem.—Eur. J.* **2002**, *8*, 3586. (b) Uemura, K.; Kitagawa, S.; Fukui, K.; Saito, K. *J. Am. Chem. Soc.* **2004**, *126*, 3817. (c) Kitaura, R.; Fujimoto, K.; Noro, S.-I.; Kondo, M.; Kitagawa, S. *Angew. Chem., Int. Ed.* **2002**, *41*, 133.

(18) Maspoch, D.; Ruiz-Molina, D.; Wurst, K.; Domingo, N.; Cavallini, M.; Biscarini, F.; Tejada, J.; Rovira, C.; Veciana, A. *J. Nat. Mater.* **2003**, *2*, 190.

(19) Li, D.; Kaneko, K. *Chem. Phys. Lett.* **2001**, *335*, 50.

(20) Takamizawa, S.; Nakata, E.-i.; Yokoyama, H.; Mochizuki, K.; Mori, W. *Angew. Chem., Int. Ed.* **2003**, *42*, 4331.

(21) Cussen, E. J.; Claridge, J. B.; Rosseinsky, M. J.; Kepert, C. J. *J. Am. Chem. Soc.* **2002**, *124*, 9574.

(22) Biradha, K.; Hongo, Y.; Fujita, M. *Angew. Chem., Int. Ed.* **2002**, *41*, 3395.

(23) Suh, M. P.; Ko, J. W.; Choi, H. J. *J. Am. Chem. Soc.* **2002**, *124*, 10976.

(24) Serre, C.; Millange, F.; Thouvenot, C.; Nogues, M.; Marsolier, G.; Louer, D.; Férey, G. *J. Am. Chem. Soc.* **2002**, *124*, 13519.

(25) Makinen, S. K.; Melcer, N, J.; Parvez, M.; Shimizu, G. K. H. *Chem.—Eur. J.* **2001**, *7*, 5176.

(26) Pan, L.; Adams, K. M.; Hernandez, H. E.; Wang, X.; Zheng, C.; Hattori, Y.; Kaneko, K. *J. Am. Chem. Soc.* **2003**, *125*, 3062.

(27) Maji, T. K.; Uemura, K.; Chang, H.-C.; Matsuda, R.; Kitagawa, S. *Angew. Chem., Int. Ed.* **2004**, *43*, 3269.

Physical Measurements. The elemental analyses were carried out on a Flash EA 112 series, Thermo Finnigan instrument. Thermal gravimetry analysis (TGA) was carried out with a Rigaku TG-8120 instrument in a nitrogen atmosphere. IR spectra were recoded on a Perkin-Elmer 2000 FTIR spectrophotometer with samples prepared in KBr pellets. X-ray powder diffraction (XRPD) data were collected on a Rigaku RINT-2200HF (Ultima) diffractometer with Cu Kα radiation. The magnetic susceptibility measurements of both the frameworks were carried out in SQUID magnetometer in the magnetic field of 1 T at the temperature range 200−2 K.

Measurement of Adsorption. The adsorption isotherm of N_2 (77 K), CO_2 (195 K), and different solvents (like H_2O, MeOH, Me_2CO, etc., at 298 K) were measured in the gaseous state by using BELSORP-18-Plus volumetric adsorption equipment from BEL, Osaka, Japan. In the sample chamber (∼17.5 mL) maintained at $T \pm 0.03$ K was placed the adsorbent sample (∼100−150 mg), which had been prepared at 423 K for **1** and 383 K for **2** and 10^{-1} Pa for about 5 h prior to measurement of the isotherms. The adsorbate was placed into the sample tube, and then the change of the pressure was monitored and the degree of adsorption was determined by the decrease of the pressure at the equilibrium state. All operations were computer-controlled and automatic.

Synthesis of $[Cu(bipy)(1,4\text{-napdc})(H_2O)_2]_n$ (1). A methanolic solution (10 mL) of bipy (1 mmol; 0.156 mg) was slowly added to the aqueous solution (15 mL) of $Cu(NO_3)_2 \cdot 2.5H_2O$ (1 mmol; 0.232 mg) with constant stirring. An instantaneous blue precipitate forms, and the mixture was stirred for 30 min. Then an aqueous solution (10 mL) of 1,4-napdcH_2 (1 mmol; 0.216 mg) and triethylamine (2 mmol; 0.204 mg) was dropwise added to the above reaction mixture, and finally the resulting solution was stirred for 2 h at 80 °C. A green compound separated quantitatively, which was filtered out, and the solution was discarded. Then the green precipitate was treated with 14% aqueous solution of NH_3 and the whole reaction mixture turned to a clear blue solution, which was kept in the open atmosphere for slow vaporization. After 2 days green single crystals suitable for X-ray structure determination were obtained, which were filtered out and washed with water. Yield: 80%. Anal. Calcd for $C_{22}H_{18}CuN_2O_6$: C, 56.23; H, 3.83; N, 5.96. Found: C, 56.29; H, 3.87; N, 6.15. IR (KBr, cm^{-1}): ν(O−H), 3548; ν_{as}(OCO), 1602; ν_s(OCO), 1350.

Synthesis of $\{([Cu(bpe)_{1.5}(1,4\text{-napdc})](H_2O)\}_n$ (2). The deep blue single crystals of **2** were obtained by adopting the same procedure only with use of bpe instead of bipy. Yield: 90%. Anal. Calcd for $C_{30}H_{24}CuN_3O_5$: C, 63.15; H, 4.21; N, 7.36. Found: C, 62.65; H, 4.54; N, 7.19. IR (KBr, cm^{-1}): ν(O−H), 3438; ν(C−H), 2926; ν_{as}(OCO), 1612; ν_s(OCO), 1378.

X-ray Crystal Structure Determination. For each of **1** and **2**, a suitable single crystal was mounted on a glass fiber and coated with epoxy resin, and X-ray data collection was carried out on a Rigaku Mercury diffractometer with graphite-monochromated Mo Kα radiation ($\lambda = 0.710\,69$ Å) and a CCD 2D detector. In both cases the sizes of the unit cells were calculated from the reflections collected on the setting angles of seven frames by changing 0.5° for each frame. Three different settings were used and were changed by 0.5°/frame, and intensity data were collected with a scan width of 0.5°. Empirical absorption correction by using REQABA was performed for all data in both cases.[28] Both the structures of **1** and **2** were solved by direct methods by using the SIR-97 program[29] and expanded by using Fourier techniques.[30] All calculations were performed with the teXsan crystallographic software package from Molecular Structure Corp.[31] For both the frameworks, the non-hydrogen atoms were refined anisotropically and all hydrogen atoms placed in the ideal positions. In **1**, the coordinated H_2O molecule shows positional disorder (O1 and O1′). The occupancy factors of O1 and O1′ were determined to be 0.65 and 0.45, respectively, on the basis of the peak heights by considering the positional overlap of hydrogen atoms. For **2,** the oxygen atom (O5) of the guest water molecules refined isotropically. Potential solvent accessible area or void space was calculated using the PLATON multipurpose crystallographic software.[32] All crystallographic and structure refinements parameters for both **1** and **2** are summarized in Table 1.

Table 1. Crystal and Structure Refinement Data for **1** and **2**

param	**1**	**2**
empirical formula	$C_{22}H_{18}CuN_2O_6$	$C_{30}H_{24}CuN_3O_5$
M_r	469.94	570.07
cryst system	monoclinic	triclinic
space group	$P2/n$ (No. 13)	$P\bar{1}$ (No. 2)
a (Å)	11.028(19)	10.613(4)
b (Å)	11.16(3)	10.828(10)
c (Å)	7.678(13)	13.333(9)
α (deg)	90.00	85.25(9)
β (deg)	103.30(5)	82.59(6)
γ (deg)	90.00	60.37(5)
V (Å^3)	919.9(3)	1320.4(17)
Z	2	2
T (K)	223	283
λ(Mo Kα)	0.710 69	0.710 69
D_c (g cm^{-3})	1.701	1.434
μ (mm^{-1})	1.235	0.873
θ_{max} (deg)	27.1	30.9
F(000)	481	588
tot. data	9773	10 810
unique data, R_{int}	2027, 0.047	6508, 0.022
data [$I > 2\sigma(I)$]	1416	5879
R^a	0.0751	0.0436
$R_w{}^b$	0.1226	0.0755
GOF	1.18	1.02

$^a R = \sum||F_o| - |F_c||/\sum|F_o|$. $^b R_w = [\sum\{w(F_o^2 - F_c^2)^2\}/\sum\{w(F_o^2)^2\}]^{1/2}$.

Results and Discussion

Synthesis. Reaction of 1,4-napdcH_2 and the organic pillar viz. bipy and bpe with Cu(II) in the presence of Et_3N produce quantitatively light green and sky blue precipitates, respectively. Both the precipitates were not soluble in any common organic solvents. Then both the compounds were dissolved in 14% NH_3 solution, resulting in the deep blue color of the solution.[33] This probably occurred due to the coordination of the NH_3 to the Cu(II) centers and the breaking of the Cu−N or Cu−O bonds. The slow evaporation of the ammoniacal solution in room temperature regenerates the

(28) Jacobson, R. A. *REQABA Empirical Absorption Correction*, version 1.1-0301998; Molecular Structure Corp.: The Woodlands, TX, 1996−1998.

(29) Altomare, A.; Burla, M. C.; Camalli, M.; Cascarano, G. L.; Giacovazzo, C.; Guagliardi, A.; Moliterni, A. G. G.; Polidori, G.; Spagna, R. *J. Appl. Crystallogr.* **1999**, *32*, 115−119.

(30) Beurskens, P. T.; Admiraal, G.; Beurskens, G.; Bosman, W. P.; deGelder, R.; Israel, R.; Smits, J. M. M. *The DIRDIF-94 Program System*; Technical Report of the Crystallography Laboratory; University of Nijmegen: Nijmegen, The Netherlands, 1994.

(31) *TeXsan Crystal Structure Analysis Package*; Molecular Structure Corp.: The Woodlands, TX, 2000.

(32) Spek, A. L. *PLATON*; The University of Utrecht: Utrecht, The Netherlands, 1999.

(33) Mukherjee, P. S.; Dalai, S.; Mostafa, G.; Zangrando, E.; Lu, T.-H.; Rogez, G.; Mallah, T.; Ray Chaudhuri, N. *Chem. Commun.* **2001**, 1346.

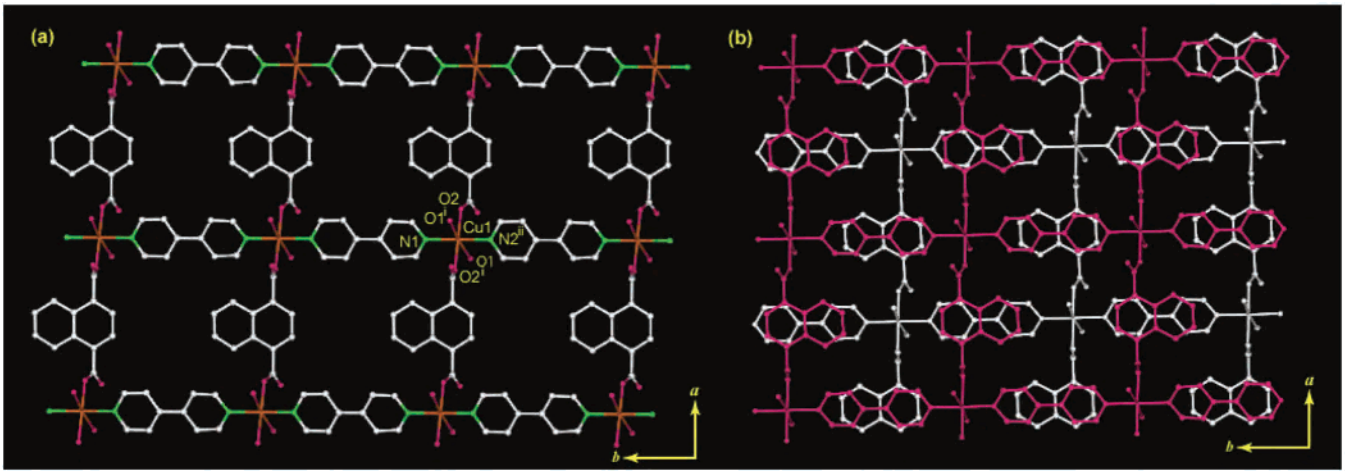

Figure 1. (a) Perspective view of the 2D rectangular grid of framework **1** lying in the crystallographic *ab* plane. (b) Perspective view along the *c*-axis of **1**, showing 2D layers stacked in a staggered manner through $\pi-\pi$ interactions. Selected bond lengths (Å) and angles (deg) for **1**: Cu1−O1, 2.541(7); Cu1−O1′, 2.506(9); Cu1−O2, 1.960(5); Cu1−N1, 2.026(6); Cu1−N2^{ii}, 2.026(6); O1−Cu1−O2, 97.0(2); O1−Cu1−N1, 93.0(1); O1−Cu1−O1^{i}, 174.0(3); O1−Cu1−O2^{i}, 83.0(2); O2−Cu1−N1, 89.7(1); O2−Cu1−O2^{i}, 179.4(2); O1−Cu1−N2^{ii}, 87.0(1); N1−Cu1−N2^{ii}, 180.0; O2^{i}−Cu1−N2, 89.7(1). (Symmetry codes: i = $-x+{}^1/_2$, y, $-z+{}^1/_2$; ii = x, $y+1$, z.)

Cu−N and Cu−O bonds. It is worth mentioning that the XRPD pattern shows the as-synthesized compound and compound after ammoniacal dissolution in the case of **1** are the same but in the case of **2** different forms generate (Figures S1 and S2). We have tried to characterize as-synthesized solid blue product in the case of **2**, but it did not materialize due to the insolubility in common organic solvents. All measurements were carried out using the sample after ammoniacal dissolution.

Structural Description of [Cu(bipy)(1,4-napdc)(H$_2$O)$_2$]$_n$ (1). The X-ray structural analysis of **1** reveals that a 2D coordination polymer of rectangular grids is built up by 1,4-napdc^{2-} and bipy ligands lying in the crystallographic *ab* plane (Figure 1a). In the (4,4) net each Cu(II) (located on a special position) is attached to two bipy, two 1,4-napdc^{2-}, and two H_2O molecules in a distorted octahedral environment. The two nitrogen atoms (N1 and N2^{ii}, Cu1−N = 2.026(6) Å) from two bipy and two oxygen atoms (O2 and O2^{i}, Cu1−O2 = 1.960(5) Å) from two 1,4-napdc^{2-} are ligated in the equatorial positions, and the trans axial sites are occupied by two oxygen atoms (O1 and O1^{i}) from two water molecules in 4 + 2 coordination with the CdN_2O_4 chromophore. The water molecules have positional disorders, O1 and O1′, with bond distances Cu1−O1 = 2.541(7) Å and Cu1−O1′ = 2.506(9) Å. The degrees of distortion from an ideal octahedral geometry are reflected from *cisoid* angles [83.0(2)−97.0(2)°] and *transoid* angles [174.0(3)−80.00°]. Each Cu(II) perfectly sits in the equatorial position without any deviation from the equatorial plane. In the 2D network, the dihedral angle between the pyridyl groups of the bipy ligand is 6.3(3)°. The Cu···Cu separations in the 2D sheet along Cu···bipy···Cu is 11.16 Å, Cu···1,4-napdc···Cu is 11.03 Å, and the effective grid dimension considering the van der Waals radii is 4.08 × 6.63 Å.[34] It is worth mentioning the adjacent sheet stack along the *c*-axis, offset by 0.5(a + b) along the *ab* plane, which facilitates the $\pi-\pi$ interactions (cg−cg distances are in the range 3.893(11)−5.309(15) Å with dihedral angle of 12.49−20.48°) between the bipy and 1,4-napdc^{2-} benzene ring, which may be responsible for the overall stabilization of the framework (Figure 1b). The nearest Cu···Cu separation between the 2D sheet is 7.66 Å.

Structural Description of {[Cu(bpe)$_{1.5}$(1,4-napdc)](H$_2$O)}$_n$ (2). X-ray structure determination reveals that the framework **2** has a unique 2D bilayer structure with molecular formula {([Cu(bpe)$_{1.5}$(1,4-napdc)](H$_2$O)}. In the 2D network each Cu(II) is pentacoordinated in a distorted square pyramidal arrangement with CuN_3O_2 chromophore, as shown in Figure 2a. Two oxygen atoms (O1, O3) belonging to two 1,4-napdc^{2-} and two nitrogen atoms (N1, N2) from two bpe moieties are ligated to the Cu(II) center in the equatorial plane, with another nitrogen atom (N3) from another bpe ligand located in the axial position. In the framework Cu1−O and Cu1−N bond distances are in the range 1.963(1)−1.972(1) and 2.030(2)−2.339(2) Å, respectively. The deviation of each Cu(II) atom from the mean plane formed by the four equatorial atom is 0.068(1) Å, and the maximum deviation of N2 below the mean plane among all the equatorial atoms is 0.037(1) Å. The degrees of distortion from an ideal square pyramidal geometry were reflected in the *cisoid* angles [87.69(7)−97.16(7)°] and *transoid* angles [173.92(7)−176.17(6)°].

All the bpe ligands adopt an anti conformation and link the Cu(II) ions into a {Cu(bpe)$_{1.5}$}$_n$ ladder as shown in Figure 2b; the bpe ligand adopts ligand conformation A (bpe^{A}), with a dihedral angle of the two pyridyl rings of 80.37(12)°, and the rungs of the ladder adopt conformation B (bpe^{B}), where the two pyridyl rings are in the same plane. The 1,4-napdc^{2-} ligand binds through the carboxylate to link the ladders into a 2D bilayer network (Figure 2c,d). The interesting feature of the structure is that the bpe^{A} and 1,4-napdc^{2-} link the Cu(II) ions into a (4,4) 2D net which is further connected by the bpe^{B} pillars forming bilayer galleries with large channels having the dimensions of 10.26 × 6.01 Å^2 [34]

(34) The size is measured by considering van der Waals radii for constituting atoms. Hereafter, all the size estimations pores are made in this way.

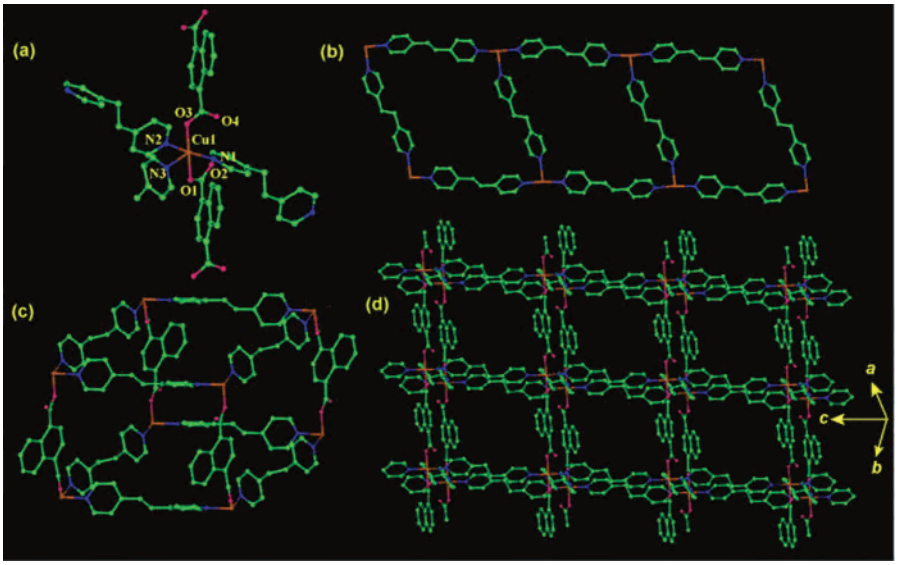

Figure 2. (a) View of the coordination environment of Cu(II) with atom-numbering scheme. (b) Perspective view of the ladder of $\{Cu(bpe)_{1.5}\}_n$ with two different conformations of the bpe ligand. (c) View of the cuboidal structural unit and (d) perspective view of the 2D bilayer network showing the rectangular channels in **2**. Selected bond lengths (Å) and angles (deg) for **2**: Cu1−O1, 1.963(1); Cu1−O3, 1.972(1); Cu1−N1, 2.042(2); Cu1−N2, 2.030(2); Cu1−N3, 2.339(2); O1−Cu1−O3, 176.17(6); O1−Cu1−N1, 92.48(7); O1−Cu1−N2, 88.91(7); O1−Cu1−N3, 87.69(7); O3−Cu1−N1, 90.34(7); O3−Cu1−N2, 88.01(7); O3−Cu1−N3, 94.96(7), N1−Cu1−N2, 173.92(7); N1−Cu1−N3, 88.82(7); N2−Cu1−N3, 97.16(7).

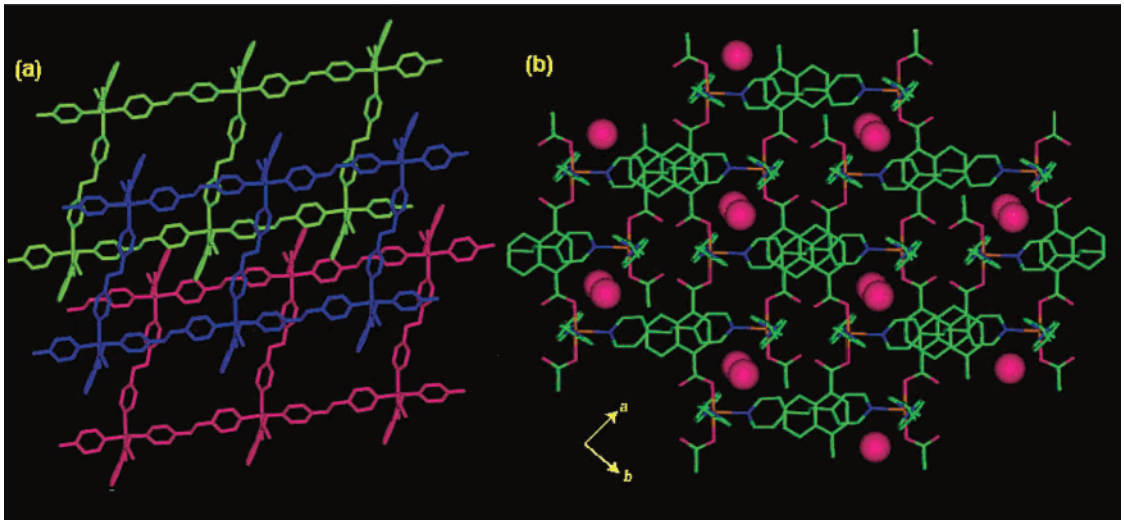

Figure 3. (a) View of the 3-fold interpenetrating 3D network. (b) Water-filled channel along the crystallographic *c*-axis in framework **2**.

(considering the van der Waals radii) (Figure 2d). In the 2D bilayer structure of **2**, a cuboidal box containing eight Cu(II) ions at the corners, connected by four 1,4-napdc^{2-} and eight long bpe linkers, making up the 12 edges, forms the fundamental building unit of **2** (Figure 2c). This cuboidal structural motif is quite different from the other bilayer structures resulted using the tetrahedral building blocks.[35]

It is worth mentioning that each bilayer network is interlocked by the two adjacent identical network (above and below) as shown in Figure 3a forming a 3-fold-interpenetrated 3D framework,[10b] which undergoes C−H$\cdots\pi$ and $\pi\cdots\pi$ interactions (cg−cg distances are in the range 3.636(4)−5.602(5) Å with dihedral angle of 0.02−28.94°). Upon interpenetration, the total effective pore size have been drastically reduces to 2.11 × 1.88 Å^2 (considering the van der Waals radii) which corresponds to the 5.2% of the total crystal volume[32] and is occupied by two water molecules (Figure 3b). The resulting 3D arrays are, therefore, an infinite catenane of decked layers of a novel interwoven framework. In the 3D network the Cu$\cdots$bpe$^A\cdots$Cu, Cu$\cdots$bpe$^B\cdots$Cu, and Cu$\cdots$1,4-napdc$\cdots$Cu distances are 13.83, 13.33, and 10.78 Å, respectively.

Thermogravimetric and XRD Analysis. To examine thermal stability of these frameworks, thermal gravimetric analysis (TGA) and X-ray powder diffraction patterns (XRPD) measurements were carried out. The TG of **1** reveals that the two coordinated water molecules release at ∼80−145 °C with color change from green to purple, and the dehydrated form is stable up to ∼235 °C and then decompose to an unidentified product (Figure S3). In case of **2** the guest water molecule release is in the temperature range ∼30−90 °C and the dehydrated framework is stable up to 230 °C

(35) Carlucci, L.; Ciani, G.; Macchi, P.; Prosperpio, D. M.; Rizzato, S. *Chem.—Eur. J.* **1999**, *5*, 237.

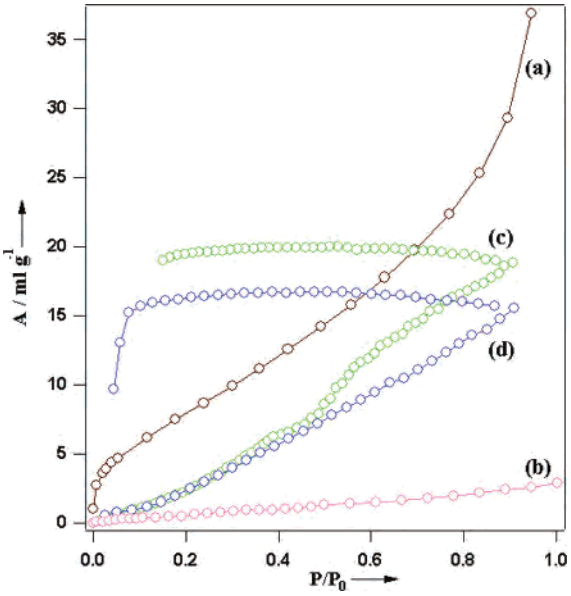

Figure 4. Isotherms for (a) N_2 (77 K), (b) CO_2 (195 K), (c) H_2O (298 K), and (d) MeOH (298 K) sorption, *A*. The P_0-saturated vapor pressure of the respective adsorbate is at indicated temperatures.

and then decompose to an unidentified product (Figure S4). No further weight loss was observed between the dehydration and the total framework decomposition in both cases. The similar XRPD patterns of as-synthesized and dehydrated forms of **1** and **2** indicate that the framework is maintained even without coordinated (for **1**) and guest water molecules (for **2**) (Figures S5 and S6). It is worth mentioning that the frameworks completely re-formed when exposed to water vapor for several hours in both cases (Figures S5 and S6).

Adsorption Properties. To examine the porosity and reactivity we have studied the adsorption property of the dehydrated frameworks of **1** and **2** with different gases (N_2, CO_2, etc.) as well as different solvent molecules (H_2O, CH_3OH, Me_2CO, etc). The sorption isotherm of N_2 (surface area = 16.3 Å^2)[36,37] at 77 K of **1** shows a type-II profile (Figure 4a), which indicates that N_2 molecules cannot diffuse into the micropore and only surface adsorption occurs. From this sorption profile, surface areas have been determined using the BET equation, which shows 43.13 m^2/g. On the other hand, H_2O (10.5 Å^2) and MeOH (18.0 Å^2) adsorption measurement shows linear increases in the pressure range (P/P_0 = 0−1 atm) without saturation and the desorption curve does not trace an adsorption one, showing large hysteresis (Figure 4c,d). This indicates that chemisorption occurs, i.e., H_2O and MeOH molecules may directly coordinated to the unsaturated Cu(II) centers. It is worth mentioning that after the H_2O and MeOH sorption the color drastically changes from purple to green, which also confirms the reaction of the H_2O and MeOH molecules with Cu(II) centers resulting in chemisorption. Conversely, the Me_2CO sorption profile suggests only surface adsorption and also

(36) Molecular area is calculated from liquid density, assuming spherical symmetry and a hexagonal close packing. The equation and values are in ref 37.

(37) Webster, C. E.; Drago, R. S.; Zerner, M. C. *J. Am. Chem. Soc.* **1998**, *120*, 5509.

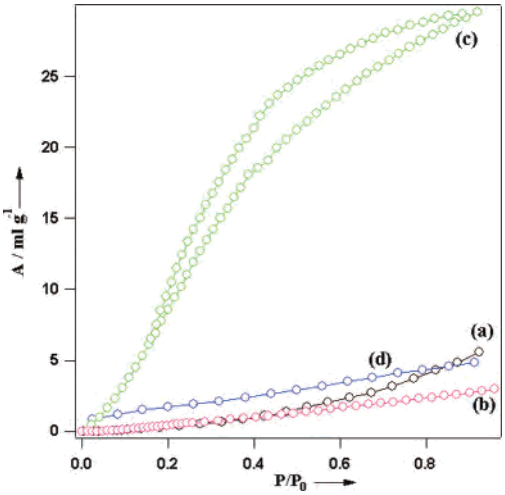

Figure 5. Isotherms for (a) N_2 (77 K), (b) CO_2 (195 K), (c) H_2O (298 K), and (d) MeOH (298 K) sorption, *A*. The P_0-saturated vapor pressure of the respective adsorbate is at indicated temperatures.

no color change was observed after exposing Me_2CO vapor. This may be due to the coordination ability of the acetone molecule being less compared to H_2O and MeOH and also the size of the Me_2CO molecules is large compared to the former two (Figure S7). The structure determination of **1** reveals that the effective pore size has been drastically reduced due to the packing of the 2D layers in a staggered manner, which prevents the diffusion of the adsorbate into the framework.

In case of framework **2**, N_2 sorption at 77 K shows only surface adsorption, suggesting no occlusion into the micropore (Figure 5a). The H_2O sorption studied reveals that H_2O molecules can diffuse inside into the micropore with hysteresis (Figure 5c) whereas MeOH molecules cannot, which shows only surface adsorption (Figure 5d). This may be due to the large size of the MeOH molecules compared to the H_2O and aperture of the channel. The micropore filling of vapors is well described by the Dudinin−Radushkevich (DR) equation:

$$\ln W = \ln W_0 - (A/\beta E_0)^2 \qquad A = RT \ln(P_0/P) \qquad (1)$$

Here, W and W_0 are the amount of adsorption at P/P_0 and the saturated amount of adsorption, respectively. A is the adsorption potential, and β and E_0 are the affinity coefficient and characteristic adsorption energy, respectively. The amount of H_2O adsorbed was calculated by the DR equation, which suggests that 0.62 molecules of H_2O are incorporated per Cu(II). The pore surface area has been calculated using the DR equation taking into account the molecular cross-section area of H_2O (0.125 nm^2), which gives the value of 84.91 m^2/g.

It is worth mentioning that both frameworks do not adsorbe CO_2 (17.9 Å^2) at 195 K (Figures 4b and 5b). This sorption selectivity in **2** is chiefly associated with the smaller channel aperture (2.11 × 1.88 Å^2), which is resulted from the 3-fold interpenetration of the 2D bilayer networks, compared to the size of the N_2, CO_2, and MeOH adsorbates.[5a]

Magnetic Properties and Magneto−Structural Correlations. The temperature dependences (300−2 K) of χ_M

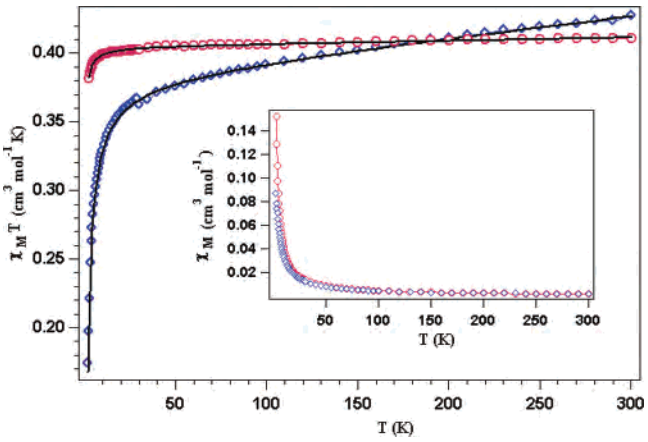

Figure 6. Plot of the $\chi_M T$ vs T (solid line showing the best fit obtained): ◇ for framework **1**; ○ for framework **2**. [Inset shows χ_M vs T (◇) for **1** and (○) for **2**.]

and $\chi_M T$ (χ_M being the magnetic susceptibility for one Cu(II) ion) for **1** and **2** are shown in Figure 6. The χ_M values of **1** and **2** at 300 K are 0.00142 cm^3 mol^{-1} ($\chi_M T = 0.427$ cm^3 mol^{-1} K) and 0.00137 cm^3 mol^{-1} ($\chi_M T = 0.411$ cm^3 mol^{-1} K), respectively, and the values are close to the expected value for a magnetically "isolated" Cu(II) ion (with $g = 2.1$). In both cases, $\chi_M T$ is almost invariable down to 100 K and gradually decreases with cooling to 2 K and there is no maxima in the χ_M vs T curve [Figure 6 (inset)]; the shapes of the $\chi_M T$ vs T curves are characteristic of the occurrence of weak antiferromagnetic interactions between the Cu(II) centers.

A $1/\chi_M$ vs T (Curie) plot in the range 2−300 K obeys the Curie−Weiss law [$1/\chi_M = (T - \Theta)C$] with Curie constant $C = 0.423$ cm^3 mol^{-1} K and Weiss temperature $\Theta = -4.470$ K for **1** and $C = 0.411$ cm^3 mol^{-1} K and $\Theta = -0.507$ K for **2**. The negative Θ value in both cases indicates (weak) antiferromagnetic interactions, in agreement with the decrease in $\chi_M T$ going to the low-temperature region. It has been already reported that the magnetic interaction through bipy and bpe ligand is negligible due to the long distances between the magnetic centers.[38] The important magnetic pathway in both structures is considered a 1D Cu(II) chain bridged by 1,4-napdc^{2-}, and thus, their magnetic behaviors can be simulated by the Bonner−Fisher uniform antiferromagnetic Heisenberg chain model. Using the effective spin Hamiltonian $H = JS_iS_{i+1}$, this takes the form of

$$\chi_M T = \frac{Ng^2\mu_B{}^2}{k_\beta} \frac{0.25 + 0.074975x + 0.075235x^2}{1.0 + 0.09931x + 0.172135x^2 + 0.757825x^3} \quad (2)$$

where $x = |J|k_\beta T$. The least-squares fit leads to the following parameters: for **1**, $J = -1.85$ cm^{-1}, $g = 2.02$, TIP = 120.0×10^{-6}, and $R = 2.43 \times 10^{-6}$; for **2**, $J = -0.153$ cm^{-1}, $g = 2.07$, TIP = 20.0×10^{-6}, and $R = 1.88 \times 10^{-7}$ (where $R = \Sigma(\chi_M T_{obs} - \chi_M T_{calc})^2/\Sigma(\chi_M T_{calc})^2$, which is actually corresponds to an excellent experiment−theory agreement).

Concerning the trend of the $-J$ values and looking at the structures of **1** and **2**, we see simple structural considerations show that the largest antiferromagnetic coupling is expected for **1**. The coordination distance of Cu(II) with the 1,4-napdc^{2-} [Cu1−O2, 1.960(5) Å] in **1** is smaller than that of **2** [Cu1−O1, 1.963(1) Å, and Cu1−O3, 1.972(1) Å]. On the other hand, in case of **1**, Cu1 does not show any deviation from the mean plane formed by the equatorial atoms, but **2** shows the deviation of 0.068(1) Å and also the angle O1−Cu1−O3 is 176.17(6)°, which is also smaller than that of **1** [O2−Cu1−O2^i, 179.4(2)°]. Thus, the energy level of the $d_{x^2-y^2}$ orbital would be different between **1** and **2,** as due to the difference of electron donation along the *z*-axis, and the orbital symmetry of **1** will be higher than that of **2**. All these structural differences correlate a stronger antiferromagnetic interaction in **1** compared to **2**, which is observed.

Concluding Remarks

In this article, we have presented the syntheses, uncommon crystallization procedure, structures, selective sorption properties, and variable-temperature magnetic properties of two novel 3D supramolecular network of Cu(II). The mixed-ligand systems such as different dicarboxylates and organic pillars are frequently used for the construction of a novel metal organic hybrid framework for the purpose to accomplish the transmission of magnetic coupling to different degrees and achieve the framework of permanent porosity and high thermal stability. In this work we use two different organic pillars (bipy and bpe) and 1,4-napdc^{2-} with Cu(II), which produce two different frameworks. The framework **1** has a 2D rectangular grid network and is stacked in a staggered manner, whereas **2** has a 2D cuboidal bilayer network and three bilayer networks mutually interpenetrated forming a 3D framework. Thus, changing the rigid spacer bipy to flexible and longer bpe causes a dramatic structural change to occur with a different network topology. This may be happening due to the lengths of the organic spacers increasing; interpenetration has been commonly adopted by Nature to avoid the formation of large open channels or cavities. The stacking of the 2D rectangular grid in a staggered manner in **1** and 3-fold interpenetration in **2** decreases the effective pore size and restrains the larger adsorbates to diffuse into the smaller channels, i.e., selective sorption, which is particularly observed in sorption experiments. Weak antiferromagnetic coupling is observed in both cases, as it is expected from their structures.

Acknowledgment. This work was supported by a Grant-In-Aid for Science Research in a Priority Area "Chemistry of Coordination Space" (No. 464) from the Ministry of Education, Science, Sports, and Culture of Japan. T.K.M. is grateful to the JSPS for a postdoctoral fellowship.

Supporting Information Available: Figures S1−S7 and X-ray crystallographic files in CIF format for **1** and **2**. This material is available free of charge via the Internet at http://pubs.acs.org.

IC050835G

(38) Mukhopadhhyay, S.; Chatterjee, P. B.; Mandal, D.; Mostafa, G.; Caneschi, A.; Slageren, J. V.; Weakley, T. J. R.; Chaudhury, M. *Inorg. Chem.* **2004**, *43*, 3413. (b) Carranza, J.; Brennan, C.; Sletten, J.; Lloret, F.; Julve, N. *J. Chem. Soc., Dalton Trans.* **2002**, 3164.